ADVANCED MATERIALS
www.advmat.de

www.MaterialsViews.com

Novel Graphene/Carbon Nanotube Composite Fibers for Efficient Wire-Shaped Miniature Energy Devices

*Hao Sun, Xiao You, Jue Deng, Xuli Chen, Zhibin Yang, Jing Ren, and Huisheng Peng**

Fiber materials play a critical role in our life. For instance, polymer fibers may represent one of the most important breakthroughs in the advancement of Materials Science, and they have been widely used as structure materials, particularly, various textiles by the well-developed weaving technology, due to the light weight and high flexibility with low cost.[1,2] In contrast, metal wires are typically explored for efficient electrode materials in a broad spectrum of electronic devices due to the high electrical conductivity.[3,4] In general, polymer fibers have been rarely investigated for electronic facilities as they are not electrically conductive, while metal wires cannot be effectively woven into applicable textile structures because of the high weight and low flexibility. However, high flexibility, strength, conductivity, and light weight are simultaneously required in many fields.

To this end, a lot of efforts have been recently made to synthesize nanostructured fibers that are proposed to achieve the above goals. In one case, carbon nanotubes (CNTs) had been spun into continuous fibers with diameters of micrometers and lengths of hundreds of meters by either dry or wet spinning processes.[5,6] Compared with the conventional fiber materials, the flexible CNT fibers showed many combined advantages including: (1) low density of 1 g/cm^3 or 10 μg/m, compared to 10 mg/m and 20–100 mg/m for cotton and wool yarns, respectively;[7] (2) high tensile strength up to 10^3 MPa with specific strength to be 5.3 times of *T1000*, the strongest commercial fiber and specific stiffness to be 4.3 times of *M70J*, the stiffest commercial fiber; (3) high electrical conductivity up to 10^3 S/cm.[8] However, the CNT fibers exhibited relatively low electrocatalytic activities that were found to be critical for electronic applications. In the other case, graphene sheets had been also made into continuous fibers.[9–14] Compared with the CNT fiber, the graphene fiber demonstrated much higher loading capability for a second phase such as platinum nanoparticles with high electrocatalytic ability but lower electrical conductivity of 10–10^2 S/cm. [9,14] Both CNT and graphene fibers had been proposed for promising electrode materials.[7,15–17]

Flexible, lightweight, portable electronic devices have continuously attracted increasing attentions and represent a mainstream direction in modern electronics.[18–20] An important breakthrough had been recently made to fabricate electronic devices in a wire format.[21] Some attempts were made to realize wire-shaped dye-sensitized solar cells, lithium ion batteries, and electrochemical supercapacitors based on CNT or graphene fibers. However, both high electrocatalytic activity and conductivity are required for these electronic devices, while they cannot be simultaneously achieved in either CNT or graphene fibers. Therefore, the photoelectric conversion efficiencies of wire-shaped solar cells and energy storage efficiencies of wire-shaped storage devices remained low.[16,22] The key to improve the above efficiencies is to develop novel fiber electrodes.

Herein, a new family of graphene/CNT composite fibers was synthesized with graphene sheets being incorporated among neighboring CNTs to serve as effective bridges to improve the charge transport because of strong π-π interactions between CNT and graphene sheet, and the novel composite fibers had simultaneously achieved both high electrical conductivity and electrocatalytic activity (**Figure 1**). As two application demonstrations, the graphene/CNT composite fiber had been used as electrodes to produce high-performance wire-shaped dye-sensitized solar cells with photoelectric conversion efficiencies up to 8.50% and supercapactiors with specific capacitances up to ~31.50 F·g^{-1} (4.97 mF·cm^{-2} or 27.1 μF·cm^{-1}), much higher than ~5.83 F·g^{-1} (0.90 ·cm^{-2} or 5.1 μF·cm^{-1}) based on the bare CNT fibers under the same condition.

To prepare the graphene/CNT composite fiber, CNT sheets were firstly drawn out of spinnable CNT arrays that had been synthesized by chemical vapor deposition (Figure S1), and

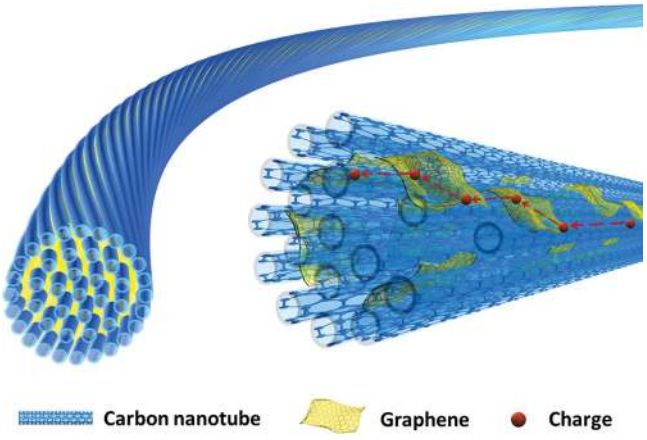

Figure 1. Schematic illustration to the structure of the graphene/CNT composite fiber. Here the transport routes indicated by the arrows are used to emphasize the fact that the bridged graphene sheets favor the charge transport, although the charges may be more easily transported along the lengths of CNTs, which are not shown for clarity.

H. Sun, X. You, J. Deng, X. Chen, Z. Yang, J. Ren, Prof. H. Peng
State Key Laboratory of Molecular Engineering of Polymers
Department of Macromolecular Science and Laboratory of Advanced Materials
Fudan University
Shanghai 200438, China
E-mail: penghs@fudan.edu.cn

DOI: 10.1002/adma.201305188

COMMUNICATION

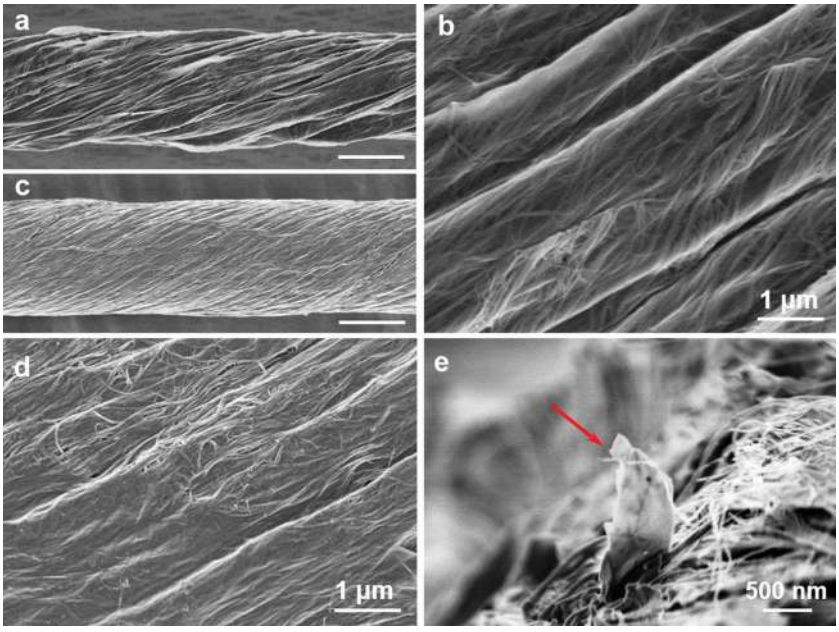

Figure 2. SEM images of graphene oxide/CNT and graphene/CNT composite fibers. a,b) A graphene oxide/CNT composite fiber at low and high magnifications, respectively. The scale bars in (a) and (c) both represent a length of 10 μm. c,d) A graphene/CNT composite fiber at low and high magnifications, respectively. e) Cross-sectional image of a graphene/CNT composite fiber at high magnifications. The arrow shows a graphene/CNT composite sheet.

then stacked along the length direction, followed by addition of 0.025 wt% graphene oxide solution (sheet widths of hundreds of nanometers to appropriately 1.5 μm, Figures S2 and S3). The as-synthesized CNT exhibited a multi-walled structure with a diameter of ~10 nm (Figure S4). The composite sheets were then twisted into graphene oxide/CNT composite fibers. Here the bare CNT sheet without graphene oxide sheets could be also twisted into fibers (Figure S5). Graphene/CNT composite fibers were produced after reduction of the graphene oxide (Figure S6). **Figures 2**a and 2b show scanning electron microscopy (SEM) images of a graphene oxide/CNT composite fiber with a diameter of ~17 μm at low and high magnifications, respectively. The graphene oxide sheets were incorporated among CNTs. After reduction of the graphene oxide, the composite fiber shrank a little as the resulting graphene sheets without oxygen-containing groups exhibited stronger π-π interactions with CNTs and among themselves (Figures 2c and 2d). The strong interactions between CNTs and graphene sheets had been also verified by high resolution transmission electron microscopy (Figure S7). Figures 2e further shows cross-sectional SEM images of the graphene/CNT composite fiber, which indicated the formation of a uniform composite.

The graphene/CNT composite fibers had been further compared with bare CNT and graphene oxide/CNT composite fibers by Raman spectroscopy (Figure S8). For a typical bare CNT fiber, G band was much larger than D band due to a high quality. After the incorporation of graphene oxide sheets, the composite fiber exhibited a larger D band compared with the G band (the intensity ratio of D to G bands to be 1.26). For the reduced graphene/CNT composite fiber, the intensity ratio of D to G bands was further increased to 1.73 due to more disordered graphene edges after elimination of pendant functional groups in graphene oxide sheets.

The graphene/CNT composite fiber showed remarkable mechanical and elecrical properties. It was flexible and could be easily made into various morphologies such as a knot without obvious fatigue in structure (**Figure 3**a). The graphene-bridged

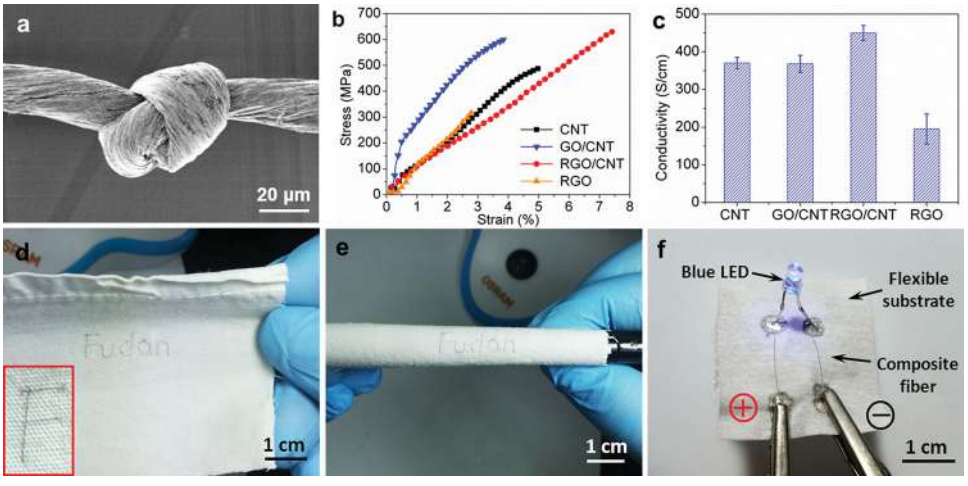

Figure 3. a) A Graphene/CNT composite fiber being made into a knot. b,c) Comparison of stress-strain curves and electrical conductivities of different fibers at room temperature, respectively. GO and RGO represent graphene oxide and reduced graphene oxide, respectively. d,e) Photographs of graphene/CNT composite fibers being woven into a flexible cotton fabric to make up a word of "Fudan". The inserted image at (d) shows the "F" at a higher magnification. f) Photographs of a blue light emission diode lamp connected to a direct-current circuit with two graphene/CNT composite fibers with length of ~1.5 cm as conducting wires. The voltage was set to 3 V.

structure also enhances the mechanical properties such as higher tensile strengths than both bare CNT and graphene fibers. Figure 3b has compared the typical stress-strain curves of bare CNT, bare graphene, graphene oxide/CNT composite and graphene/CNT composite fibers under the same experimental condition. For a bare CNT fiber, the tensile strength was ~500 MPa. For the graphene oxide/CNT composite fiber, it was increased to ~610 MPa as the graphene oxide sheet served as cross-linking components to stabilize the neighboring CNTs. After reduction of the graphene oxide, the tensile strength had been further improved to ~630 MPa as graphene sheets can more effectively interact with CNTs due to the stronger π-π interactions to transfer the load[9–11]. A relatively lower tensile strength of ~320 MPa was obtained from bare graphene fibers.

The electrical conductivities of the above fibers at room temperature had been also compared in Figure 3c. A bare CNT fiber exhibited a conductivity of (370 ± 15) S/cm. After incorporation of graphene oxide sheets, the conductivities remained almost unchanged, i.e., (368 ± 22) S/cm. As expected, the reduced graphene/CNT composite fiber showed much increased conductivity of (450 ± 20) S/cm. Individual CNTs showed low electrical resistances, and the relatively high resistances of CNT fibers were mainly derived from high contact resistances among CNTs. The introduction of insulating graphene oxide sheets among CNTs almost did not affect the charge transport, so the conductivities were not obviously changed. In contrast, graphene sheets served as conducting "bridges" to decrease the contact resistances. Bare graphene fibers demonstrated conductivities of (195 ± 40) S/cm[9,10] or ~400 S/cm.[11,12]

The graphene/CNT composite fibers were flexible but tough, and they could be easily woven into various fabrics. As a demonstration, Figure 3d exhibits a photograph of composite fibers being woven into a piece of cotton fabric to form a word of "Fudan". The resulting fabric had been bent or scrolled into desired morphologies with stable structures (Figure 3e). Due to the high conductivity, the graphene/CNT composite fiber had been also used as effective conducting wires (Figures 3f). Two composite fibers served as conducting wires to connect a blue light emission dioxide (LED) lamp with a direct-current power. The lamp could be stably operated without any fatigue in the illumination after 5000 cycles.

To further demonstrate the high performances, the graphene/CNT composite fibers had been compared with bare CNT, graphene, and graphene oxide/CNT composite fibers as counter electrodes to fabricate effective dye-sensitized solar cells in a unique wire format. Figure S9 shows a SEM image of a typical cell with a TiO_2 nanotube-modified Ti wire as the working electrode. The cyclic voltammographs had been firstly studied in **Figure 4**a. Two pairs of oxidation/reduction peaks were observed with the left pair corresponding to the redox reaction of I_3^-/I^-. In general, a counter electrode with higher catalytic activity shows a smaller peak-to-peak voltage separation (V_{pp}) in the cyclic voltammogram. Compared with bare CNT fiber, the graphene/CNT composite fiber exhibited a relatively lower catalytic activity. However, the graphene/CNT composite fiber could be uniformly deposited with small Pt nanopariticles (diameters of ~10 nm) due to the existence of graphene sheets on the surface. The resulting graphene/CNT/Pt composite fiber showed a low V_{pp} of 0.32 V with high catalytic activity. In contrast, it was

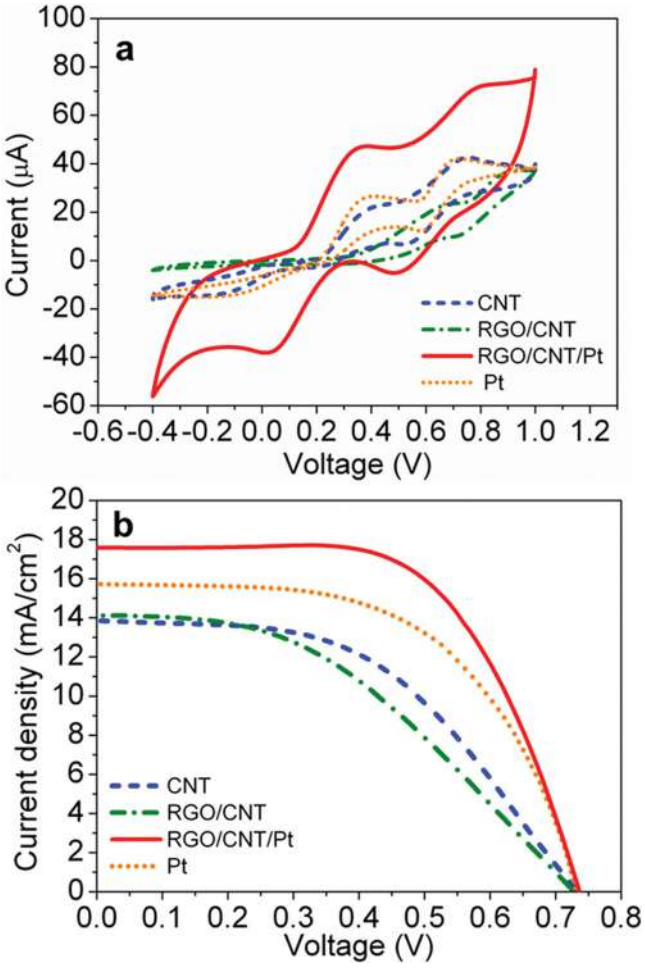

Figure 4. a) Comparison on electrochemical properties of bare CNT, graphene/CNT, graphene/CNT/Pt and bare Pt fibers, respectively. b) Comparison on J-V curves of wire-shaped DSCs with bare CNT, graphene/CNT, graphene/CNT/Pt and bare Pt fibers as the counter electrodes, respectively.

much less effective to deposit Pt nanoparticles onto the smooth bare CNT fiber, and Pt nanoparticles tended to form larger aggregates with diameters of ~200 nm (Figure S10).

A smaller V_{pp} indicated the a higher activity of the counter electrode to catalyze the redox reaction of I_3^-/I^-, which contributed to a higher energy conversion efficiency of the dye-sensitized solar cell.[23] Figure 4b has compared J-V curves of wire-shaped dye-sensitized solar cells based on bare CNT and graphene/CNT composite fibers before and after deposition of Pt nanoparticles. The graphene/CNT composite fiber exhibited a higher Jsc but lower FF than the bare CNT fiber due to a higher conductivity and lower catalytic activity of the composite fiber. As a result, the graphene/CNT composite fiber showed a lower energy conversion efficiency of (4.30 ± 0.10)%, compared to (5.03±0.12)% for the bare CNT fiber. However, after deposition of Pt nanoparticles, the graphene/CNT/Pt composite fiber showed energy conversion efficiencies of (8.36 ± 0.10)%. It should be noted that, for a bare Pt wire, energy conversion efficiencies of (6.66 ± 0.15)% were achieved.

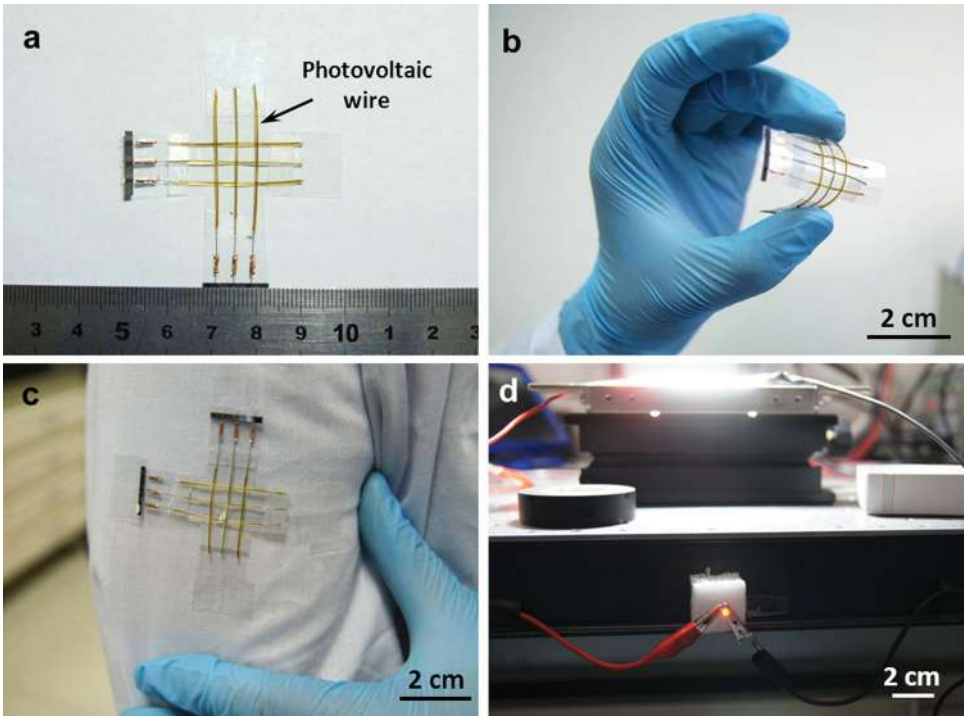

Figure 5. A photovoltaic textile woven from 6 wire-shaped solar cells. a,b) Photographs of the photovoltaic textile before and after bending, respectively. c) The photovoltaic textile attached onto a flexible coat. d) A commercial red light emission diode lamp lightened up by the photovoltaic textile. The photovoltaic textile was operated under illumination of simulated AM1.5 solar light from a solar simulator.

These wire-shaped solar cells could be easily woven into lightweight and flexible textiles for practical applications. **Figure 5**a shows a photovoltaic textile fabricated from six wire-shaped solar cells. As expected, it had exhibited stable and high energy conversion efficiencies under bending (Figures 5b and S11). The photovoltaic textile could be further integrated into clothes or attached onto various flexible substrates to power miniature devices (Figures 5c and 5d). As an application demonstration, a commercial red light emission diode lamp had been lighted up by the photovoltaic textile (Figure 5d). Such photovoltaic textiles are particularly useful to support portable and flexible devices or facilities in the future.

These conducting fibers had been further twisted to make wire-shaped micro-capacitor (Figures S12 and S13). **Figure 6**a has compared the bare CNT and graphene oxide/CNT composite fibers by cyclic voltammetry. A typical rectangular shape corresponding to a double layer capacitor was found for the bare CNT fiber, while a redox peak at 0.3–0.6 V that indicated a pseudo-capacitance derived from the oxygen-containing functional groups had been observed for the graphene oxide/CNT composite fiber. Galvanostatic charge-discharge curves based on bare CNT and graphene oxide/CNT composite fibers are also compared in Figure 6b. The bare CNT fiber exhibited a symmetrical triangle for the electric double–layer capacitor, while the graphene oxide/CNT composite fiber showed a deviation from the triangle, which was derived from rapid Faradaic reactions in the presence of oxygen-containing groups, particularly, epoxy and alkoxy in graphene oxide sheets.[24–26] Figure 6c further shows galvanostatic charge-discharge curves of wire-shaped capacitors on the basis of graphene oxide/CNT composite fibers at increasing current densities of 0.2, 0.4, 1.0 and 2.0 A/g. All the curves remained the symmetrical shapes, indicating a high reversibility during the charge and discharge processes in a wide current range. The electrochemical stability of the wire-shaped capacitor was further analyzed by cyclic voltammetry at increasing scan rates of 10, 50, 100, 200 $mV \cdot s^{-1}$ (Figure 6d). The rectangular shape had been well maintained for a good electrochemical stability.

The dependence of specific charge and discharge capacitance on current density was also compared in Figure 6e. The maximal specific capacitance achieved ~31.50 $F \cdot g^{-1}$ (4.97 $mF \cdot cm^{-2}$ or 27.1 $\mu F \cdot cm^{-1}$) at a current density of 0.04 A/g, compared with ~5.83 $F \cdot g^{-1}$ (0.90 $\cdot cm^{-2}$ or 5.1 $\mu F \cdot cm^{-1}$) based on the bare CNT fibers under the same condition (Figure S14). Therefore, the capacitances were not obviously changed with the varying GO content in the composite fiber. Electrochemical impedance spectroscopy was also used to characterize the micro-capacitor (Figure S15). The 90° inclination in the Nyquist plot indicated a nearly perfect capacitor performance. The semi-arc from the inserted image further demonstrated a pseudo-capacitance derived from the graphene oxide. The horizontal inception corresponded to the equivalent series resistance of 11.0 $Ohm \cdot cm^2$. The wire-shaped capacitor derived from the graphene oxide/CNT composite fiber showed a high cyclic stability (Figure 6f). No obvious decrease in capacitance had been observed in 5000 cycles.

In summary, novel nanostructured composite fibers based on graphene and CNT have been developed with high tensile strength, electrical conductivity, and electrocatalytic activity. As two application demonstrations, these composite fibers

ADVANCED MATERIALS
www.advmat.de

www.MaterialsViews.com

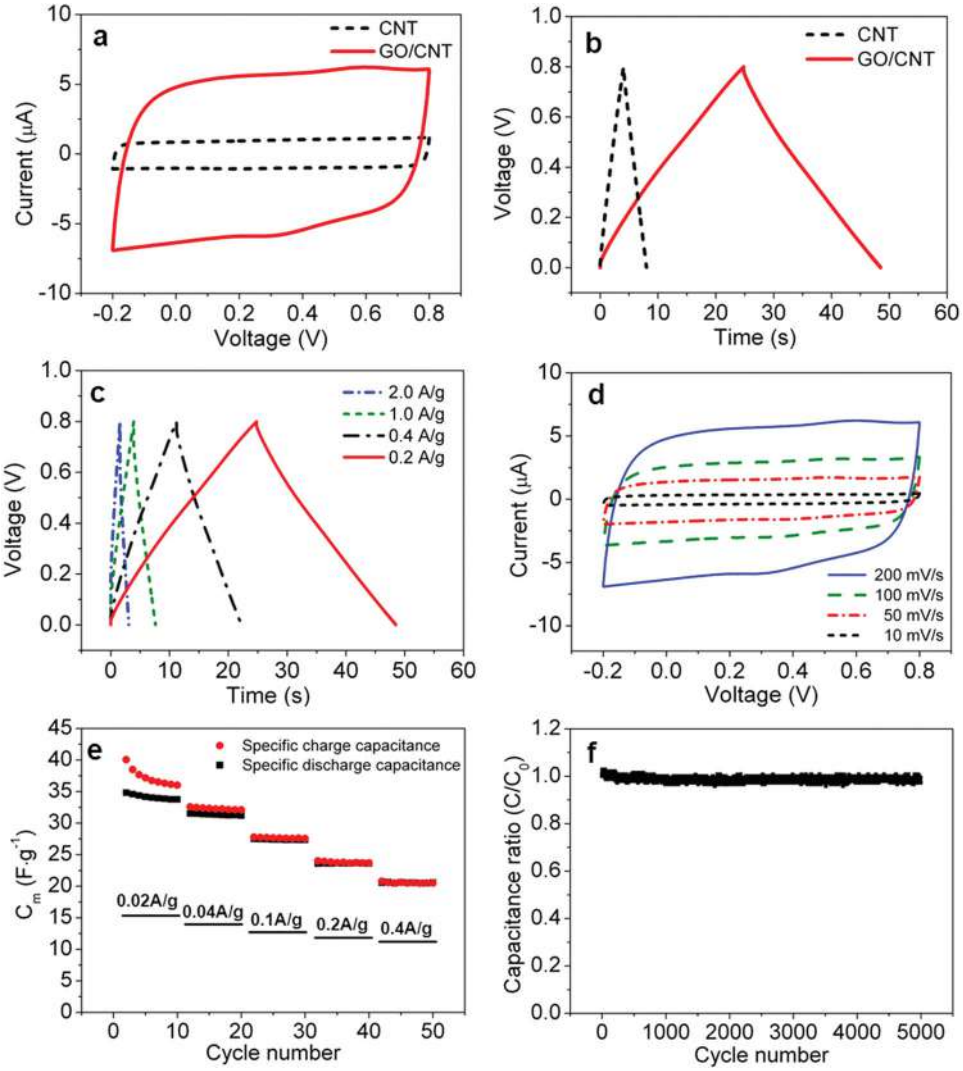

Figure 6. a,b) CV and galvanostatic charge-discharge curves of wire-shaped supercapacitors with bare CNT and graphene oxide/CNT composite fibers as electrodes, respectively. The CV and galvanostatic charge-discharge curves were measured at 200 $mV \cdot s^{-1}$ and 1×10^{-6} A, respectively. The wire-shaped supercapacitors showed the same length of 1.2 cm. c, d) Galvanostatic charge-discharge and CV curves based on the graphene oxide/CNT composite fiber electrodes at increasing current densities and scan rates, respectively. e) Dependence of specific capacitance on current density. f) Dependence of specific capacitance on cycle number based on the graphene oxide/CNT composite fiber electrode. The specific capacitance was calculated from the charge-discharge curves at a current density of 2.0 A/g.

are used to fabricate flexible, wire-shaped dye-sensitized solar cells and electrochemical supercapacitors both with high performances. The wire-shaped dye-sensitized solar cell shows a maximal energy conversion efficiency of 8.50%, and the wire-shaped supercapacitor exhibits a high specific capacitance of ~31.50 $F \cdot g^{-1}$ (5.83 $F \cdot g^{-1}$ derived from bare CNT fibers). These miniature wire-shaped devices have been further shown to be promising for flexible and portable electronic facilities.

Experimental Section

Synthesis of composite fibers. The synthesis of CNT array and graphene oxide is described in the Supporting Information. Graphene oxide/CNT composite fibers were fabricated by a biscrolling method.[15] Briefly, CNT sheets that had been drawn out of the CNT array were stacked along the length direction,[27] followed by addition of the graphene oxide solution (0.025 wt%) in water and ethanol (volume ratio of 1:20). The resulting graphene oxide/CNT composite films were scrolled into fibers at the rotary rate of 2000 rpm. Graphene/CNT fibers could be further synthesized by dipping the graphene oxide/CNT fibers in an aqueous solution of hydroiodic acid (40%) at 80 °C for 6h, followed by immersion into methanol and drying in vacuum for 12 h.

Deposition of Pt nanoparticles. A double potential step method was used to deposit Pt nanoparticles onto the surfaces of bare CNT and graphene/CNT composite fibers at room temperature with the first step at –0.5 V for 5 s and the second step at 0 V for 30 s.[28] The electrolyte was composed of 5 mM H_2PtCl_6 and 0.5 M H_2SO_4 in water, and a platinum wire and saturated calomel electrode served as counter and reference electrodes (+0.241 V vs. RHE), respectively. The resulting fibers were immersed in deionized water to remove the electrolyte and dried in vacuum for 12 h.

Fabrication of wire-shaped dye-sensitized solar cells. A TiO_2 nanotube-modified Ti wire that absorbed N719 dye served as the working

electrode.[29] The dye-absorbed working electrode was twisted with a composite fiber as the counter electrode to form a wire-shaped dye-sensitized solar cell. The wire-shaped solar cell could be sealed in a transparent flexible fluorinated ethylene propylene tube, followed by injection of a redox electrolyte (containing 0.1 M lithium iodide, 0.05 M iodine, 0.6 M 1, 2-dimethyl-3-propylimidazolium iodide, and 0.5 M 4-tert butyl-pyridine in dehydrated acetonitrile and 2-dimethyl-3-propylimidazolium iodide).

Fabrication of wire-shaped supercapacitors. The graphene/CNT composite fiber electrodes were firstly incorporated with a gel electrolyte of PVA/H_3PO_4 (mass ratio of 1/1) and dried in vacuum. The resulting two fiber electrodes were then twisted together, followed by coat of a second layer of the same gel electrolyte to avoid the short circuit of the wire-shaped supercapacitor.

Supporting Information

Supporting Information is available from the Wiley Online Library or from the author.

Acknowledgements

This work was supported by NSFC (91027025, 21225417), MOST (2011CB932503, 2011DFA51330), STCSM (11520701400, 12nm0503200), Fok Ying Tong Education Foundation, the Program for Professor of Special Appointment at Shanghai Institutions of Higher Learning, and the Program for Outstanding Young Scholars from Organization Department of the CPC Central Committee.

Received: October 18, 2013
Revised: December 2, 2013
Published online: January 25, 2014

[1] F. Vollrath, D. P. Knight, *Nature* **2001**, *410*, 541.
[2] Z. Xu, C. Gao, *Macromolecules* **2010**, *43*, 6716.
[3] W. Kylberg, F. A. De Castro, P. Chabrecek, U. Sonderegger, B. T. T. Chu, F. Nüesch, R. Hany, *Adv. Mater.* **2011**, *23*, 1015.
[4] X. Fan, Z. Chu, F. Wang, C. Zhang, L. Chen, Y. Tang, D. Zou, *Adv. Mater.* **2008**, *20*, 592.
[5] A. B. Dalton, S. Collins, E. Munoz, J. M. Razal, V. H. Ebron, J. P. Ferraris, J. N. Coleman, B. G. Kim, R. H. Baughman, *Nature* **2003**, *423*, 703.
[6] N. Behabtu, C. C. Young, D. E. Tsentalovich, O. Kleinerman, X. Wang, A. W. Ma, E. A. Bengio, R. F. ter Waarbeek, J. J. de Jong, R. E. Hoogerwerf, *Science* **2013**, *339*, 182.
[7] T. Chen, S. Wang, Z. Yang, Q. Feng, X. Sun, L. Li, Z. S. Wang, H. Peng, *Angew. Chem. Int. Ed.* **2011**, *50*, 1815.
[8] X. Zhang, Q. Li, T. G. Holesinger, P. N. Arendt, J. Huang, P. D. Kirven, T. G. Clapp, R. F. DePaula, X. Liao, Y. Zhao, *Adv. Mater.* **2007**, *19*, 4198.
[9] Z. Xu, C. Gao, *Nat. Commun.* **2011**, *2*, 571.
[10] X. Hu, Z. Xu, C. Gao, *Sci. Rep.* **2012**, *2*. 767.
[11] Z. Xu, H. Sun, X. Zhao, C. Gao, *Adv. Mater.* **2013**, *25*, 188.
[12] Z. Xu, Z. Liu, H. Sun, C. Gao, *Adv. Mater.* **2013**. *25*, 3249.
[13] C. Xiang, C. C. Young, X. Wang, Z. Yan, C. C. Hwang, G. Cerioti, J. Lin, J. Kono, M. Pasquali, J. M. Tour, *Adv. Mater.* **2013**. *25*, 4592
[14] Z. Dong, C. Jiang, H. Cheng, Y. Zhao, G. Shi, L. Jiang, L. Qu, *Adv. Mater.* **2012**, *24*, 1856.
[15] M. D. Lima, S. Fang, X. Lepró, C. Lewis, R. Ovalle-Robles, J. Carretero-González, E. Castillo-Martínez, M. E. Kozlov, J. Oh, N. Rawat, *Science* **2011**, *331*, 51.
[16] J. Ren, L. Li, C. Chen, X. Chen, Z. Cai, L. Qiu, Y. Wang, X. Zhu, H. Peng, *Adv. Mater.* **2013**. 25, 1155.
[17] Y. Meng, Y. Zhao, C. Hu, H. Cheng, Y. Hu, Z. Zhang, G. Shi, L. Qu, *Adv. Mater.* **2013**, *25*, 2326.
[18] M. Kaltenbrunner, M. S. White, E. D. Głowacki, T. Sekitani, T. Someya, N. S. Sariciftci, S. Bauer, *Nat. Commun.* **2012**, *3*, 770.
[19] M. S. White, M. Kaltenbrunner, E. D. Głowacki, K. Gutnichenko, G. Kettlgruber, I. Graz, S. Aazou, C. Ulbricht, D. A. Egbe, M. C. Miron, *Nat. Photonics* **2013**. *7*, 811.
[20] Y. Kim, J. Zhu, B. Yeom, M. Di Prima, X. Su, J.-G. Kim, S. J. Yoo, C. Uher, N. A. Kotov, *Nature* **2013**, *500*, 59.
[21] T. Chen, L. Qiu, Z. Yang, H. Peng, *Chem. Soc. Rev.* **2013**. *42*, 5031.
[22] T. Chen, L. Qiu, H. G. Kia, Z. Yang, H. Peng, *Adv. Mater.* **2012**, *24*, 4623.
[23] A. Hagfeldt, G. Boschloo, L. Sun, L. Kloo, H. Pettersson, *Chem. Rev.* **2010**, *110*, 6595.
[24] B. Xu, S. Yue, Z. Sui, X. Zhang, S. Hou, G. Cao, Y. Yang, *Energy Environ. Sci.* **2011**, *4*, 2826.
[25] E. Raymundo-Piñero, M. Cadek, F. Beguin, *Adv. Funct. Mater.* **2009**, *19*, 1032.
[26] Q. Bao, S. Bao, C. M. Li, X. Qi, C. Pan, J. Zang, Z. Lu, Y. Li, D. Y. Tang, S. Zhang, *J. Phys. Chem. C* **2008**, *112*, 3612.
[27] W. Wang, X. Sun, W. Wu, H. Peng, Y. Yu, *Angew. Chem. Int. Ed.* **2012**, *124*, 4722.
[28] M. Duarte, A. Pilla, J. Sieben, C. Mayer, *Electrochem. Commun.* **2006**, *8*, 159.
[29] H. Sun, X. You, Z. Yang, J. Deng, H. Peng, *J. Mater. Chem. A* **2013**, *1*, 12422.